SAMPLING STRATEGIES TO ENABLE COMPUTATIONALLY EFFICIENT SPACE-RIP FOR 3D PARALLEL MR IMAGING

W. Scott Hoge[1], Lei Zhao[1], Dana H. Brooks[2], and Walid Kyriakos[1]

(1) Dept. of Radiology, Brigham and Women's Hosp. and Harvard Medical School, Boston, MA. USA
(2) Electrical and Computer Engineering Dept., Northeastern University, Boston, MA. USA

ABSTRACT

New MR acquisition techniques are enabling fast acquisition of data from an entire 3D volumes. Parallel MR imaging methods can provide additional acceleration to the data acquisition rate. However, the large computational memory requirements associated with 3D imaging requires new efficient reconstruction techniques. This manuscript presents an efficient implementation of SPACE-RIP for the rapid reconstruction of sub-sampled 3D MR data. Uniform sub-sampling effectively decouples the SPACE-RIP linear system of equations into a number of smaller systems which can each be solved independently, thus requiring fewer computational resources. We present a particular phase-encode sampling pattern to capitalize on this effect which allows SPACE-RIP to be computationally competitive with SENSE in 3D imaging, while providing the added benefits of self-calibrated coil sensitivity maps and improved artifact suppression through irregular sub-sampling.

1. INTRODUCTION

In the pursuit of reduced MR image acquisition times, a number of image reconstruction methods have been proposed. Parallel imaging methods achieve this goal by distributing the data acquisition burden across multiple receiver coils and then sub-sampling during data acquisition to reduce the total image acquisition time. The strength of these reconstruction methods is the ability to suppress aliasing artifacts in the reconstructed image that arise from sub-sampling along the phase-encode dimension.

To reconstruct an image from sub-sampled multi-coil data, SPACE-RIP [1] constructs a large linear system of equations. The large number of parameters in the linear system gives SPACE-RIP greater freedom in reconstruction regularization approaches and an unlimited choice of phase encode lines to acquire. This is significant because reconstructions from variable density data have significantly fewer aliasing artifacts than images formed from uniform down-sampled data. Variable density phase-encoding also allows one to obtain self-referenced coil sensitivity estimates for use in reconstruction.

The penalty for solving such a large system of equations is high computational cost. In the particular case of 3D MR imaging, the SPACE-RIP linear system can be prohibitively large — often exceeding the physical memory capacity of most (reasonably priced) modern computer systems. In this work, we use the fact that uniform sub-sampling of the phase-encoding decouples the SPACE-RIP linear system into a group of smaller, independent systems. We have shown earlier [2] that this decoupled form of SPACE-RIP is in fact analytically equivalent to the popular SENSE [3] method.

In 3D imaging, this decoupling allows the SPACE-RIP problem to again be reduced to a number of smaller problems. In this manuscript, we describe a method to reduce the computational load of 3D SPACE-RIP, by efficiently solving the system constructed with irregular sub-sampling along one phase encode direction, and uniform down-sampling along the other. We demonstrate that the combination of irregular and uniform sub-sampling respectively along two phase encoding dimensions provides significantly better aliasing artifact suppression compared to 2D SENSE for 3D imaging [4] at the same speedup factor, while maintaining comparable reconstruction times.

2. METHODS

All parallel MR imaging methods aim to reconstruct an image of the excited spin distribution from down-sampled data acquired using multiple coils. The signal acquired in each coil, l, can be described by

$$s_l(\mathbf{k}) = \int_V W_l(\mathbf{r})\rho(\mathbf{r})e^{j2\pi\mathbf{k}\cdot\mathbf{r}}d\mathbf{r} + \eta(\mathbf{k}). \qquad (1)$$

where $\rho(\mathbf{r})$ is the excited spin density function throughout the volume V, $\mathbf{r}$ is the spatial position in the field of view (FOV), $W_l(\mathbf{r})$ is the coil sensitivity at point $\mathbf{r}$, $\mathbf{k}$ is a reciprocal spatial term corresponding to the gradients employed

Grant support provided by NIH T32-EB002177 and NIH R21-EB000567-02

during data acquisition, $\mathbf{k} = \gamma \int_0^\tau \mathbf{G}(t)dt$, and $\eta(\mathbf{k})$ is additive noise in the received signal.

This signal representation is typically discretized to solve the inverse problem computationally. As originally presented, Cartesian SENSE [3] imposes a uniform downsampling pattern. Based on the subsequent aliasing pattern, one can then construct a small system for each spatial-domain pixel in the acquired data reference frame. Solving this small system gives un-aliased spatial-domain pixels. This process is then repeated for each pixel in the FOV. In Space-RIP [1], an FFT is performed along one dimension to consider each column of the FOV in turn. This results in a large linear system

$$\bar{s} = \mathbf{P}\bar{\rho} + \bar{\eta} \tag{2}$$

where the vector $\bar{s}$ contains the output data from all coils for a single column, $\bar{\rho}$ is one column in the (reconstructed) image, $\bar{\eta}$ represents additive noise, and $\mathbf{P}$ is a system matrix constructed from knowledge of the phase-encoding pattern used and the coil sensitivity estimates. As with any linear system, one can alternatively frame the reconstruction as a minimization problem

$$\min_{\bar{\rho}} \|\bar{s} - \mathbf{P}\bar{\rho}\|_2, \tag{3}$$

with the possibility of adding regularization terms as well. One can take the derivative of this cost function to yield the associated *normal equations*.

$$\mathbf{P}^H\bar{s} = \mathbf{P}^H\mathbf{P}\bar{\rho}. \tag{4}$$

Below, we use this normal equations representation of the parallel MR image reconstruction problem to expose effects of various sub-sampling choices on the analytic structure of the problem.

2.1. The structure of the SPACE-RIP matrix

In 2D MR imaging, the SPACE-RIP linear system, $\bar{s} = \mathbf{P}\bar{\rho}$, can be described by [2]

$$\begin{bmatrix} s_1(:,x) \\ s_2(:,x) \\ \vdots \\ s_L(:,x) \end{bmatrix} = \begin{bmatrix} P^H \mathrm{diag}\{W_1(:,x)\} \\ P^H \mathrm{diag}\{W_2(:,x)\} \\ \vdots \\ P^H \mathrm{diag}\{W_L(:,x)\} \end{bmatrix} \rho(x,:). \tag{5}$$

where associated with each coil l, there is a length M vector of acquired data, $s_l(:,x)$, corresponding to particular column x in the reconstructed image, and an N-by-N diagonal matrix, $\mathrm{diag}\{W_l(x,:)\}$, which contains the coil sensitivity estimate, $W_l(x,:)$, associated with column x along the main diagonal. The elements of the M-by-N matrix P^H correspond to the exponential term in (1), $P(n,k_y) = e^{-jk_y n\tau}$, where each row of P^H corresponds to a particular phase encode k_y. We note here that the columns of P (and rows of P^H) correspond to columns of the discrete Fourier transform operator, and are mutually orthogonal.

In the case of 3D imaging, the SPACE-RIP system matrix, $\mathbf{P}$, can again be represented compactly as a stack of matrices, each of the form

$$\left[(Q^H \otimes P^H)\mathrm{diag}\{\mathrm{vec}\{W_l\}\}\right] \tag{6}$$

where W_l is the spatial sensitivity estimate for coil l *for the entire slice*, and the rows of Q^H and P^H correspond to the Fourier encoding harmonic terms, $e^{j\gamma(G_r^h n\tau)}$, induced by phase encode h and gradient direction G_r. $\otimes$ refers to the Kronecker product. In 3D imaging, phase-encoding occurs along two dimensions of the FOV, and Q^H and P^H each correspond to the sampling pattern along one of those phase encoding dimensions.

2.2. Uniform sub-sampling and the normal equations

As was originally shown in [2], the normal equations perfectly illustrate the aliasing operator that results when phase-encode sub-sampling is employed. Consider the following 2D example. Using the system matrix in Eq. (5) for $\mathbf{P}$, one finds

$$\mathbf{P}^H\mathbf{P} = \left[(PP^H) \circ \left(\sum_{l=1}^{L} W_l(:,x) W_l(:,x)^H \right) \right] \tag{7}$$

where $\circ$ represents an element-by-element matrix product. In this form, the interaction between the selected phase encodes and the coil sensitivities is readily apparent. The outer product PP^H acts as a projection matrix onto the subspace defined by the selected phase encodes.

Thus, when uniform sub-sampling by the f, the system matrix

$$\mathbf{P}^H\mathbf{P}\Big|_{\text{2D uniform}} = [(\mathbf{1}_f \otimes I_{N/f}) \circ (\sum_{l=1}^{L} W_l(:,x) W_l(:,x)^H)] \tag{8}$$

can be permuted into a block diagonal matrix. Each block of this permuted normal-equations representation can be solved independently. We refer to this result as a *decoupling* of the normal equations system matrix through the use of uniform sub-sampling. We have shown previously in [2] that this decoupled form is analytically equivalent to the Cartesian SENSE [3] method for sub-sampled parallel MR data reconstruction.

In the case of irregular sub-sampling along the phase encode direction, this decoupling behavior no longer exists. The structure of PP^H gains significant complexity and one is unable to permute $\mathbf{PP}^H$ into a block diagonal matrix. Thus, in the case of irregular sub-sampling, it is advantageous to examine each column in the 2D image reconstruction problem as a single large system. Creating a large system matrix effectively captures the impact of the sub-sampling pattern employed, its effect on the data acquisition process, and gives greater freedom in regularization and greater control of aliasing artifacts. Thus, there is significant motivation to study irregular sub-sampling approaches. In the case of 3D imaging, the combination of irregular and uniform sub-sampling along two separate coordinate axes provides a significant benefit as we demonstrate below.

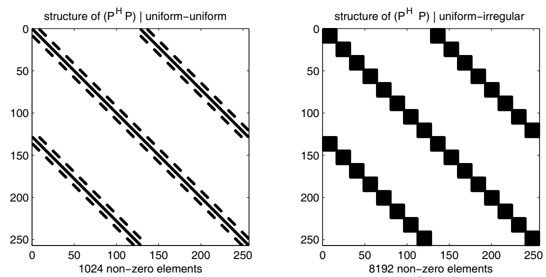

Fig. 1. Structure of normal equations when uniform sub-sampling is employed along (a) both phase encoding directions, and (b) only one phase encoding direction.

2.3. Decoupling the 3D problem

In the case of 3D imaging, one can employ this decoupling effect along either or both phase-encoded dimensions. In the case of uniform down-sampling along both phase encode directions, the normal equations system matrix becomes:

$$\mathbf{P}^H\mathbf{P}\Big|_{\text{3D uniform}-\text{uniform}} = \Big[((\mathbf{1}_f \otimes I_{m/f}) \otimes (\mathbf{1}_g \otimes I_{n/g})) \circ (\sum_{l=1}^{L} \text{vec}\{W_l\}\text{vec}\{W_l\}^H)\Big],$$

whose sparse structure is shown in Fig. 1(a). It is this linear system structure that 2D-SENSE [4] exploits to reconstruct 3D parallel data. Similarly, employing irregular down-sampling along one phase encode direction and uniform down-sampling in the other, the block-matrix structure is retained, but each block looses the $(\mathbf{1}_g \otimes I_{n/g})$ structure present before. Specifically,

$$\mathbf{P}^H\mathbf{P}\Big|_{\text{3D uniform}-\text{irregular}} = \Big[\Big((\mathbf{1}_f \otimes I_{m/f}) \otimes (PP^H)\Big) \circ (\sum_{l=1}^{L} \text{vec}\{W_l\}\text{vec}\{W_l\}^H)\Big].$$

The sparsity structure of this matrix is given in Fig. 1(b) for the case of a 16-by-16 pixel image, sub-sampled by 2 along each phase encode direction. Computational savings result from the fact that the solution to each of these decoupled systems can be found independently, then be used collectively to solve the complete 3D SPACE-RIP linear system.

3. RESULTS

We demonstrate this approach on full 3D volume four-coil data acquired on a 1.5T GE Signa MR scanner with coils arranged circumferentially around the volunteers head. To test our 3D SPACE-RIP reconstruction methods using various different sampling patterns, 1-by-1-by-1 mm^3 isotropic resolution images covering the entire 3D FOV were acquired using a high-resolution 3D Fast Spin Echo sequence [6]. with no acceleration. The acquisition required 10.4 minutes to fill a 160-by-192-by-256 *k*-space cube with data samples. To allow reasonable time for a full 3D SPACE-RIP reconstruction, one axial slice from this *k*-space data was selected, and sub-sampled by 2 to form a 80 pixel by 86 pixel reference image.

Our efficient image reconstruction approach was tested by exchanging an irregular sub-sampling for uniform sub-sampling along both phase encode directions. The irregular sampling pattern employed a phase encode selection guided by the relative energy density in *k*-space, sampling densely at the lower *k*-space frequencies and more sparsely at the high frequencies.

The acquisition speed-up factor (4x) was equivalent in all cases. Fig. 3 shows the reconstruction and aliasing artifacts present for reconstructions of simulated acqusition data for (a) a uniform-uniform, (b) irregular-uniform, and (c) irregular-irregular sub-sampling strategies. For reference, the full resolution image in shown in Fig. 2. The aliasing artifacts present in each reconstruction are shown to the right of the reconstructions, normalized to the maximum artifact level of all three images. Note that the use of irregular sampling significantly reduces the appearance of aliasing artifacts.

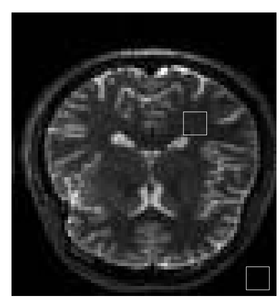

Fig. 2. Image reconstructed with no acceleration. Boxes show the regions used for the SNR estimation in all reconstructed images.

On a SUN Ultra-80 with 4GB RAM, the 2D-SENSE reconstruction of case (a) required 28.1 sec. The computation time to reconstruct the efficient SPACE-RIP case (b) was longer, 74.7 sec, but significantly shorter than the time to solve the full SPACE-RIP problem (c), 7228.7 sec ($\approx$ 2 hours).

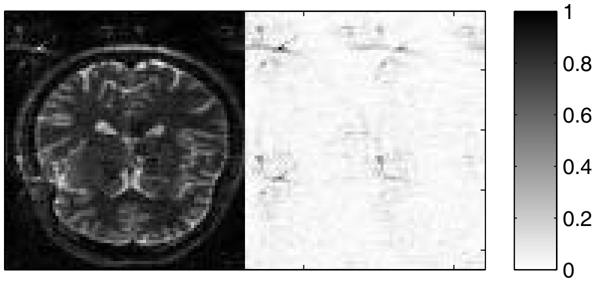

(a)

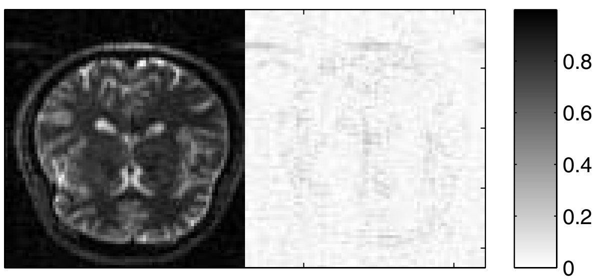

(b)

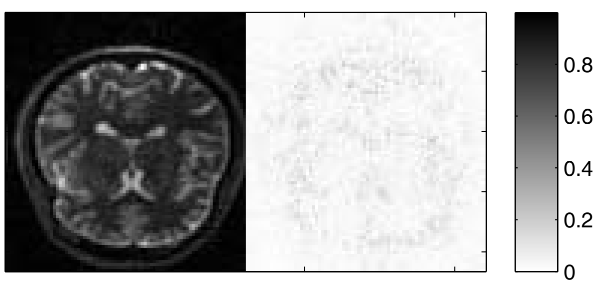

(c)

Fig. 3. SPACE-RIP Image reconstructions based on (a) uniform-uniform, (b) irregular-uniform, and (c) irregular-irregular downsampling patterns.

Note that the use of irregular downsampling improves SNR performance. To measure SNR, following the method in [8], two 7-by-7 pixel regions were selected (shown in Fig. 2): one covering tissue, and one outside the tissue region. The location of the boxes was chosen based on relatively uniform signal intensity *and* the absence of significant aliasing artifact. The ratio of signal power to noise was estimated by calculating the mean intensity of the pixels in the tissue-covering-box, divided by the standard deviation of the signal intensity in the null-signal-box. The table below displays the estimated SNR for each of the reconstructed images. Clearly, irregular downsampling improves the SNR of the reconstructed image.

Phase-encode sampling pattern	SNR
uniform-uniform	6.935126
irregular-uniform	13.330072
irregular-irregular	19.931803
no acceleration	66.219387

Estimated SNR for each reconstruction method.

4. SUMMARY

We have presented an efficient SPACE-RIP implementation for the rapid reconstruction of multi-coil 3D FSE data. Using the fact that uniform downsampling effectively decouples the SPACE-RIP linear system of equations,we propose using a hybrid phase-encoding pattern to capitalize on this effect in 3D MR imaging: irregular sub-sampling along one dimension and uniform sub-sampling along the second phase encode dimension. Each of the small decoupled systems formed by this downsampling pattern can be each solved independently requiring a significantly smaller computational footprint. This approach allows SPACE-RIP to be computationally competitive with SENSE in 3D MR imaging. This choice of phase encoding pattern provides the added benefits of improved artifact suppression from irregular downsampling and allows the use of self-calibrated coil sensitivity estimates if desired.

5. REFERENCES

[1] W. E. Kyriakos, L. P. Panych, et. al., "Sensitivity profiles from an array of coils for encoding and reconstruction in parallel (SPACE RIP)," *Magn. Reson. Med.*, vol. 44, no. 2, pp. 301–308, Aug. 2000.

[2] W. S. Hoge, D. H. Brooks, et. al., "On the regularization of SENSE and Space-RIP in parallel MR imaging," in *Proc. IEEE Int. Symp. on Biomedical Imaging (ISBI04)*, pp. 241–244, Apr. 2004.

[3] K. P. Pruessmann, M. Weiger, et. al. "SENSE: Sensitivity encoding for fast MRI," *Magn. Reson. Med.*, vol. 42, no. 5, pp. 952–62, Nov. 1999.

[4] M. Weiger, K. P. Pruessmann, and P. Boesiger, "2D SENSE for faster 3D MRI," *MAGMA*, vol. 14, no. 1, pp. 10–9, Mar. 2002.

[5] P. C. Hansen, *Rank-Deficient and Discrete Ill-Posed Problems*. SIAM Press, 1998.

[6] L. Zhao, J. Mugler, et. al. "A high-resolution clinical whole-brain scan using single-slab three-dimensional T1W, T2W and FLAIR fast spin-echo sequences," in *Proc. ISMRM* 10^{th} *Scientific Meeting*, (Honolulu, Hawai'i, USA), p. 1294, ISMRM, May 2002.

[7] N. Aggarwal and Y. Bresler, "Optimal sampling in parallel magnetic resonance imaging," in *Proc. of IEEE Intl. Conf. on Image Processing (ICIP-03)*, vol. II, (Barcelona, Spain), pp. 831–834, 14-17 Sep. 2003.

[8] E. M. Haacke, R. W. Brown, M. R. Thompson, and R. Venkatesan, *Magnetic Resonance Imaging: Physical Principles and Sequence Design*. John Wiley and Sons, 1999.